Building Tomorrow's Society
Bâtir la Société de Demain

Fredericton, Canada
June 13 – June 16, 2018/ *Juin 13 – Juin 16, 2018*

STRENGTH PREDICTION OF UHPFRC-FILLED CLOSURE STRIP BETWEEN PRECAST BRIDGE DECK SLABS INCORPORATING RIBBED-SURFACE GFRP BARS

Ndreko, Ilion[1,4], Sennah, Khaled[2], Sennah, Hosam[3]
[1,2,3] Ryerson University, Toronto, Canada
[4] indreko@ryerson.ca

Abstract: In accelerated bridge construction, the use of glass fiber reinforced polymer (GFRP) bars as internal reinforcement in concrete is a viable option for the expedited replacement of deteriorated concrete bridge deck slabs, where corrosion of steel reinforcement is of main concern. This research investigates the use of ribbed-surface GFRP bars in the closure strip between jointed precast deck slabs resting over steel or concrete girders and seeks to determine the effects of concrete strength at the joint. The jointed deck slab utilizes two vertical shear keys, one on each side of the closure strip. GFRP bars in the precast slabs project with straight ends into the closure strip, which is then filled with ultra-high performance fibre-reinforced concrete (UHPFRC) of 150 MPa compressive strength. Six full-scale specimens with dimensions of 200x600x2800 mm and different non-contact bar splice lengths, namely; 75, 105, 135 and 165 mm were tested to failure under four-point load. The anchorage behavior is observed and recorded to evaluate the manner in which the capacities of the non-contact straight-end GFRP bars are developed. Values for optimal girder spacing related to joint width and GFRP embedment length are computed for standard dead and live loading.

1 INTRODUCTION

Bridges are some of the most vital and important transportation structures linking our world together. Maintaining such an important structure by ensuring its safety and serviceability is beneficial to the well-being of our communities both socially and economically. In Canada the deterioration of steel reinforced concrete bridges is expedited through the corrosion of the reinforcing bar. This corrosion is caused by the usage of de-icing salts, which break down the passive layer in the reinforcing bar, and the high temperature fluctuations between day & night or between the different seasons, which cause severe cracking in the concrete. Bridge decks are usually some of the most affected by this type of deterioration as they are the first component to make contact with this severe environment. The emergence of glass-fiber reinforced polymer bars has become a prominent replacement material for steel bars in reinforced concrete due to their corrosive resistant properties. On the other hand, municipalities often struggle to replace severely deteriorated bridge components in time or find the budget to repair and maintain this infrastructure. This is why it is important for decision makers not only to ensure that durability and service life of the new materials far exceeds that of their counterparts but to also find cost-effective ways to replace deteriorated components quickly. For larger cities and communities, where construction delays have a big impact on their ecosystem, accelerated bridge construction (ABC) has become one of the go-to methods of construction for the replacement of bridge components. The federal highway administration (FHWA) defines accelerated bridge construction as making use of innovative planning, design, materials, and construction methods, in a safe and cost-effective manner, to reduce the onsite construction time that occurs when building new bridges or

replacing/rehabilitating existing bridges (Culmo 2009). ABC results in improved site constructability, while ensuring enhanced project delivery time and work zone safety for travelling public. It also reduces the impact on traffic, and weather-related time delays, while maintaining and/or improving construction quality. All these benefits result in reduced life cycle cost and decreased environmental impact. During construction, prefabricated components can be delivered to site and quickly assembled, and thus they can reduce construction time and cost through minimized formwork usage, shorter lane closure times, and possibly eliminate the need for a temporary bridge. Recent surveys of the state of practice of full-depth, full-width panel-girder system and joints were conducted elsewhere (PCI, 2011; NCHRP, 2011; Badie and Tadros, 2008). Few authors have dealt with panel-to-panel longitudinal joints in bulb-tee girder (Sennah and Afifi, 2015, Afefy et al., 2015; Li et al., 2011; Graybeal, 2010). While others authors have dealt with panel-to-panel transverse joints (Culmo, 2011; Graybeal, 2010). Zhu et al. (2012) proposed continuous transverse U-bar joint details, incorporating projecting reinforced steel bars from the jointed panels which can provide negative moment continuity in multi-span bridges, however no pretensioning was used. One of the ABC techniques is the use of prefabricated systems to minimize the use of the conventional cast-in-place techniques. A major component of such system, which is the focus of this research, is the jointed prefabricated deck panels that are supported over either steel or prefabricated precast concrete girders. Figure 1 depicts a schematic diagram of precast full-depth deck panels placed transversally over girders. Figure 2 shows several bulb-tee pretensioned girders placed side-by-side and jointed together at the level of the deck slab.

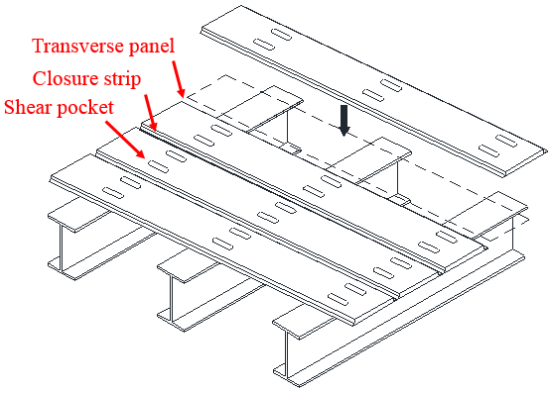

Figure 1: Transverse prefabricated panels over steel girders

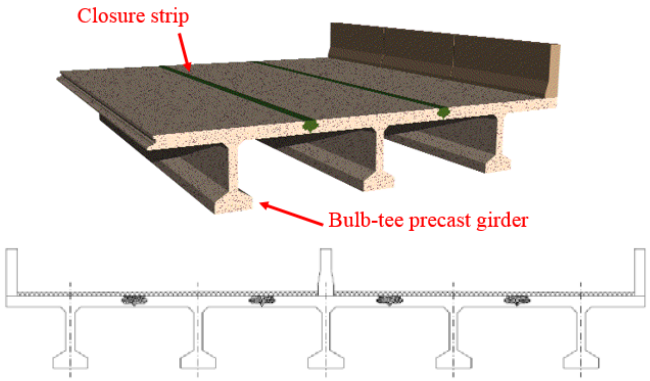

Figure 2: Bulb-tee precast girders jointed together at the deck

2 SIGNIFICANCE OF THIS RESEARCH

Several research studies been conducted on the behavior of the joint between the precast prefabricated deck panels considering conventional steel reinforcement, epoxy-coated steel bars and GFRP bars. Summary of these studies can be found elsewhere (Culmo, 2009; Khalafalla and Sennah, 2015; Sayed Ahmed and Sennah, 2016). These studies investigated the reinforcement details in the joint such as bent bars, bars with hooked ends, straight and headed-end bars, combined with different shear key shapes and different joint filling materials, such as non-shrinking grout, high performance concrete (HPC) and ultra-high performance fiber reinforced concrete (UHPFRC). Among the materials being proposed and investigated in the jointed precast deck panels, the ribbed-surface GFRP bars and UHPFRC are of a growing interest and focus. The outstanding properties of each of these materials eliminate the durability issues that existed when using steel reinforcement and allow for expansion on accelerated bridge construction practice. However, literature survey showed that neither the Canadian Highway Bridge Design Code (CHBDC, 2014) nor the AASHTO-LRFD Specifications for Design of Highway Bridges (AASHTO-LRFD, 2012) provide guidance for the design of the joints of prefabricated deck slabs reinforced with GFRP and UHPFRC. Also, the most recently developed AASHTO Bridge Design Guide Specifications for GFRP-Reinforced Concrete Bridge Decks and Traffic Railings (AASHTO, 2009) does not provide guidance on the design of closure strips between GFRP reinforced precast deck panels. Therefore, this research was established to provide guidance for the design of such jointed slabs when subjected to dead loads and truck live loads. The

proposed experimental program provides data to assist in obtaining the precast deck slab capacity based on the joint details as affected by joint width and associated bar splice length.

3 RESEARCH OBJECTIVES

The objective of this research was to conduct a parametric study using experimental testing to investigate the behavior of ribbed-surface GFRP bars in the closure strip between jointed precast deck slabs resting over steel or concrete girders. The experimental findings are then correlated with the available theoretical moment and shear capacities of the slab cross-section to examine their applicability. Finally, for design purposes, the maximum spacing between girders to be considered to use the developed joints in practice were determined based on CHBDC applied factored dead and live load moments.

4 EXPERIMENTAL PROGRAM

4.1 Test Parameters

This experimental study was composed of a control group 1 with continuous bars in order to compare with the slabs in group 2 which are made of non-contact GFRP bars with various splice lengths. The slabs had a fixed spacing of bars in the lap splice and main bar spacing with bar splice length of 75, 105, 135 and 165 mm for closure strip widths of 125, 155, 185 and 215 mm, respectively as per Table 1. It should be noted that target compressive strengths of precast concrete and UHPFRC were 35 and 150 MPa, respectively.

Table 1: Test Matrix

Group	Slab dimensions (mm)	Slab No.	Joint Width	Splice Length	f'_c (MPa)		Splice Configuration		Bar spacing (mm)
					Regular Concrete	UHPC Joint	Type	Offset (mm)	
1	2800×600×200	S1	-	-	35 MPa	-	-	N/A	200
		S2	185	-	35 MPa	150 MPa			
2	2800×600×200	S3	125	75	35 MPa	150 MPa	Non-contact	100	200
		S4	155	105					
		S5	185	135					
		S6	215	165					

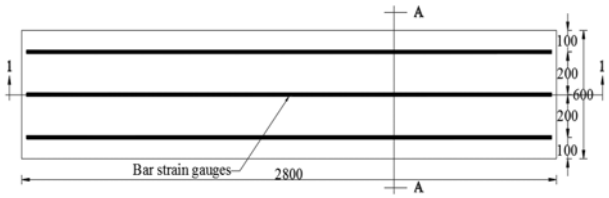

Figure 3: Top view of slab S1 with continuous bars

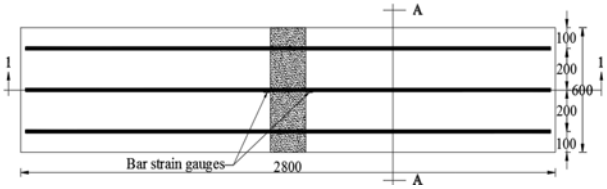

Figure 4: Top view of slab S2 with shear key and continuous bars

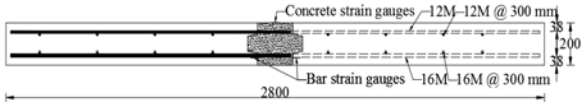

Figure 5: Side view of all Group 2 Slabs

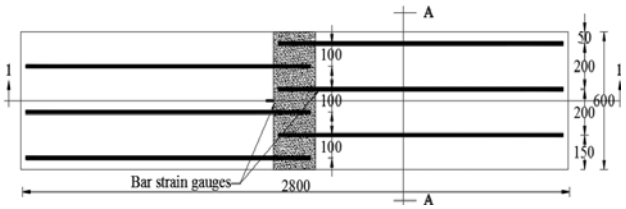

Figure 6: Top view of all Group 2 slabs

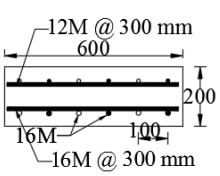

Figure 7: Group 2 Section A-A

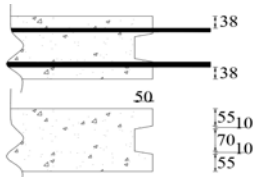

Figure 8: Shear Key Dimensions

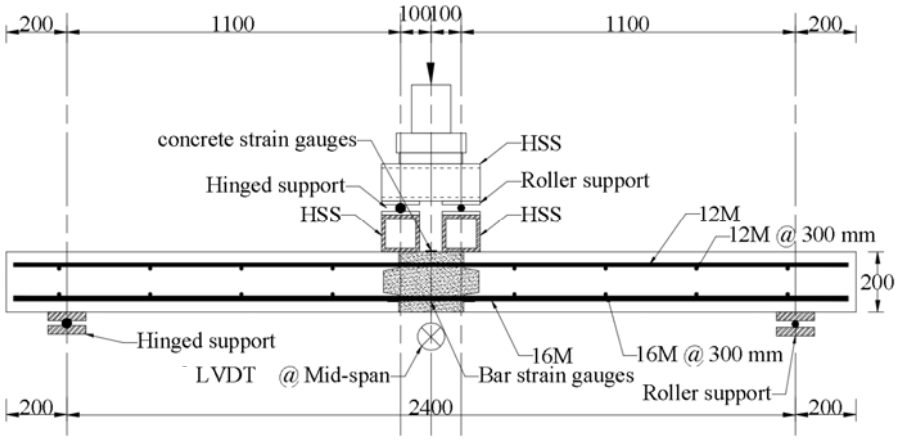

Figure 9: Test setup for all slabs

Each of the tested slabs had a 2800 mm total length and 2400 mm effective span length between supports. The slab thickness and width are 200 and 600 mm, respectively, as depicted in Figures 3-7. Test specimens in group 2 considered non-contact lap splice where the spacing between the two bars in the lap splice is 100 mm (Figure 6). The main tension reinforcement located at the bottom in all slabs was composed of 16M GFRP bars. The widths of the closure strip were taken as 125, 155, 185 and 215 mm for slabs S3, S4, S5, and S6, respectively, on which the projecting bar length stopped 25 mm short of the joint width to allow for construction tolerance. The shape of the joint is a typical shear key as depicted in Figure 7. The tensile strength and modulus of elasticity of the bars were 1188 MPa and 64 GPa, respectively, tensile strain at rupture of 1.86% (Schoeck, 2013). Two bar sizes were considered in this study, namely: 12M and 16M bars with nominal cross-sectional area of 113 and 201 mm^2, respectively. The main tension reinforcement and bottom transverse reinforcement the slabs were considered of 16M bar, while 12M bars were used for the top reinforcement. A four-point loading test setup was used in this study in order to expose the joint to pure flexure (Figure 9). Each slab was simply-supported over steel pedestals. A hinged support was utilized at the left support line using a steel rod sandwiched between two grooved steel plates while at the right support line, a roller support was formed on top of the pedestal using a steel rod sandwiched between two flat steel plates. Three linear variable displacement transducers (LVDTs) were installed at the mid-span to measure the deflection. The load was applied gradually in increments of 10 kN until failure so that initiation of cracks and crack propagation were recorded. A data acquisition system was used to collect data from strain gauges and the load actuator during the test.

5 EXPERIMENTAL RESULTS

Concrete cylinder specimens were tested to-collapse at the time of each test to determine the average compressive strength of normal-strength concrete as well as UHPFRC. Table 2 summaries the results from these tests for each slab.

Table 2: Concrete Compressive Strength at Day of Testing

Slab Number	Compressive Strength (f'_c)	
	Regular Concrete Strength (MPa)	***UHPFRC Joint Strength (MPa)***
S1	49.60	N/A
S2	50.36	152.43
S3	49.56	151.91
S4	50.33	149.78
S5	51.09	155.43
S6	49.34	142.66

5.1 Failure Modes and Results Description

The jointed slab S1 with 35 MPa regular concrete and continuous bars was tested to-collapse. The first flexural crack was observed starting at the bottom right directly below the applied load at 23.48 kN. This crack continued propagating upward along the interface of the joint and the precast slab with increase in applied load. Other flexural-shear cracks within the precast slab started to appear between the one-third points of the slab at around 30 kN and continued propagating towards the top of the slab causing flexural-shear failure at an ultimate load of 140.19 kN. View of crack pattern at failure for specimen S1 is shown in Figure 10 & 12. Slab S2 with shear key and continuous bar was tested to collapse under the same type of loading. The first flexural crack was observed at the interface between the precast concrete and the UHPFRC-filled joint at 13.64 kN. This crack continued propagating upward along the interface of the joint and the precast slab with increase in applied load up to 130 kN. Other flexural and shear cracks within the precast slab started to appear just outside of the shear key between 40-60 kN and continued propagating towards the top of the slab causing flexural-shear failure at an ultimate load of 140.36 kN. (Figure 10 & 12). Jointed slab S3 with splice length of 75 mm and joint width of 125 mm was tested to-collapse. The first flexural crack was observed at the interface between the precast concrete and the UHPFRC-filled joint at 9.19 kN. This crack continued propagating upward along the interface of the joint and the precast slab with increase in applied load. Other flexural cracks within the precast slab started to appear just outside the joint and continued propagating towards the top of the slab with increase of applied load until pure flexural failure at 76.21 kN. Jointed slab S4 with splice length of 105 mm and joint width of 155 mm was tested to-collapse. The first flexural crack was observed at the interface between the precast concrete and the UHPFRC-filled joint at 12.46 kN and continued to propagate to the top until a pure flexural failure occurred at a load of 93.64 kN. Similarly, jointed slab S5 with a lap splice length of 135 mm and joint width of 185 mm started cracking at 8.40 kN on the UHPFRC joint and regular concrete interface and propagated until full flexural failure occurred at 120.10 kN. Finally, jointed slab S6 with a splice length of 165 mm and joint width of 205 mm initially started to crack at a load of 7.04 kN at the UHPFRC-Regular Concrete joint interface. The crack propagated mainly on one side of the joint until full failure occurred at a load of 117.66 kN. Major regular concrete spalling occurred as a result of bar slippage near the interface and on the bottom of the slab (Figure 11 & 13). None of the slabs suffered any damage on the UHPFRC joint itself.

Table 3: Summary of Failure Modes and Ultimate Loads

Group	Slab	Ultimate Load	Ultimate Moment	Ultimate Shear	Cracking Load	Cracking Moment	Failure Mode
		kN	*kN·m*	*kN*	*kN*	*kN·m*	
1	**S1**	140.19	77.11	70.10	23.48	12.91	Flexural-Shear
	S2	140.27	77.15	70.14	13.64	7.50	Flexural-Shear
2	**S3**	76.21	41.92	38.11	9.19	5.06	Flexural
	S4	93.64	51.50	46.82	12.46	6.85	Flexural
	S5	120.10	66.06	60.05	8.30	4.57	Flexural
	S6	117.66	64.71	58.83	7.04	3.87	Flexural

From Table 3, one may observe that flexural-shear failure mode occurred in Group 1 slabs with continuous bars. While all Group 2 slabs had a pure flexural failure. When comparing results for slabs S3 and S4 of the same failure mode, it can be observed that the increase of splice length from 75 to 105 mm increased the slab capacity by 23%. Also, when comparing results for slabs S4 and S5, it can be observed that the increase of splice length from 105 to 135 mm increased the slab capacity by 28%. When comparing results for slabs S5 and S6, it can be observed that the increase of splice length from 135 to 165 mm showed slight decrease in the load carrying capacity of 2% while the failure mode remained unchanged. The slight difference of 2% may be attributed to the difference in compressive strength of the UHPFRC joint as depicted in Table 2. It can be concluded that the load carrying capacity of the slab may remain unchanged for an increase in splice length beyond 135 mm and hence the joint width beyond 185 mm. In all Group 2 slabs, one may observe that the flexural crack at the interface between the UHPFRC and the precast slab was too wide to the extent that bar slip from the UHPFRC occurred. To investigate this hypnosis, a core sample was taken from each slab and then sliced at the bar location to examine whether the bar slipped

from concrete. Figures 14 & 15 show views of the sliced core sample showing the end of the GFRP bar slipped from concrete at its end as well as shearing of bar ribs, respectively.

Table 4: Summary of Ultimate Loads Compared to Group 1 Slabs

Group	Slab	Ultimate Load *kN*	Load Compared to S1	Load Compared to S2
1	**S1**	140.19	100.00 %	99.94 %
	S2	140.27	100.06 %	100.00 %
2	**S3**	76.21	54.36 %	54.33 %
	S4	93.64	66.80 %	66.76 %
	S5	120.10	85.67 %	85.62 %
	S6	117.66	83.93 %	83.88 %

Figure 10: Group 1 Side 1

Figure 11: Group 2 Side 1

Figure 12: Group 1 Side 2 Close Up

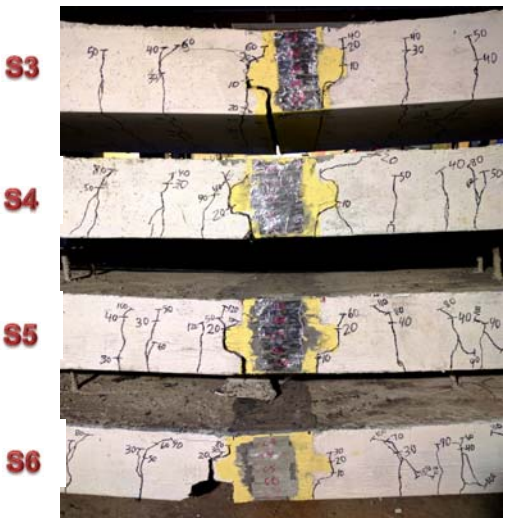

Figure 13: Group 2 Side 2 Close Up

Figure 16 depicts the applied moment-deflection relationship for the tested slabs. It can be observed that the maximum deflection increases with larger joint widths when failure mode is flexural. Figure 19 shows the relationship between the applied moment and the maximum concrete strain at top of the slab. One may observe that the maximum concrete strains for all Group 2 slabs, which failed in flexure, does not exceed 1200 με. These values are far below the concrete failure micro-strain of 3500, confirming the flexural failure resulted from bar slip from UHPFRC in the closure strip and rib shearing as depicted in Figure 14. Figure 18 depicts the relationship between the applied moment and bar strain at the joint-precast slab interface. One may observe that the maximum strain values were 1.08%, 1.28%, 1.4% and 1.48% for slabs S3, S4, S5 and S6, respectively. The corresponding failure stresses on the bars were 691, 819, 896 and 947 MPa for slabs S1, S2, S3 and S4, respectively.

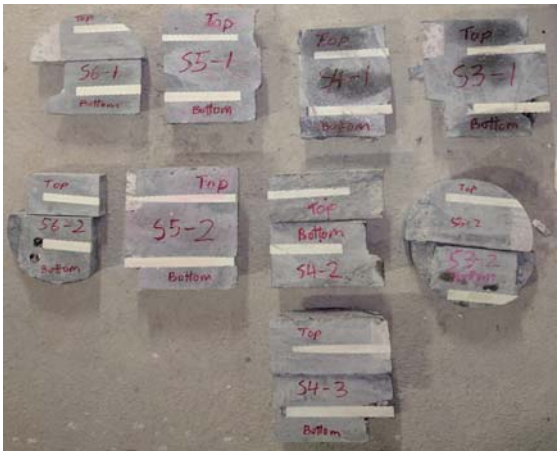

Figure 14: View of GFRP bar slippage

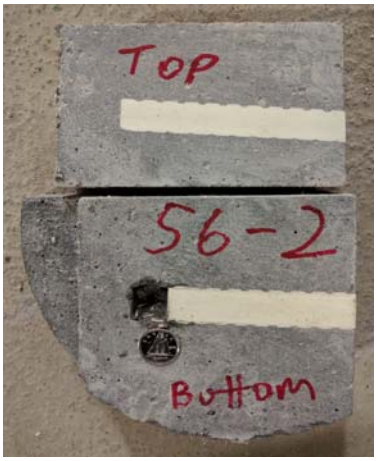

Figure 15: View of bar slippage failure in slab S6 due to shearing of the bar ribs and bar slip

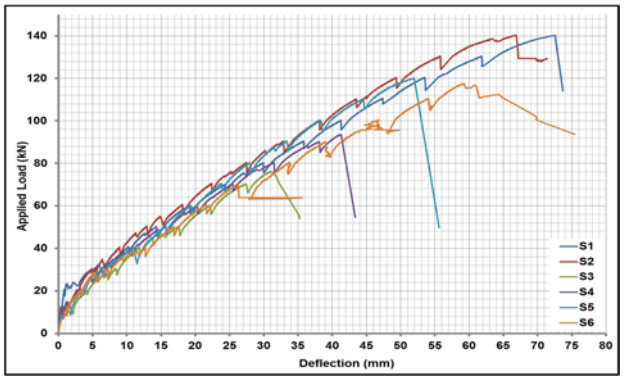

Figure 16: Moment vs deflection relationship for all tested slabs

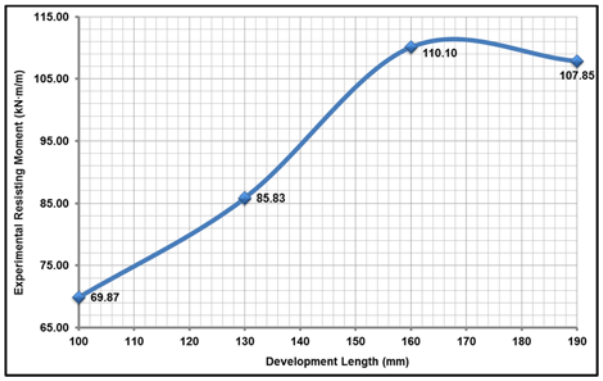

Figure 17: Moment and GFRP development length relationship

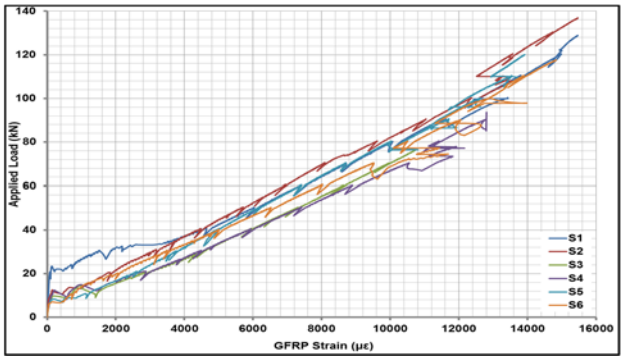

Figure 18: Load vs GFRP strain relationship for the tested slabs

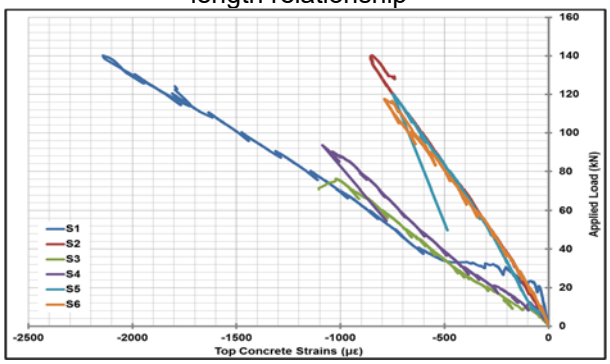

Figure 19: Load vs top concrete strains for all slabs

5.2 Theoretical Moment and Shear Capacities

Theoretical moment and shear capacities for the precast slabs were calculated based on ISIS Canada manual No. 3 (ISIS, 2007) and CHBDC of 2014. The capacities were calculated using spreadsheets programed based on the equations and procedures presented in the above-mentioned references. These capacities were obtained considering resistance factors for concrete and GFRP bars of 0.75 and 0.55, respectively. However, the experimental capacity requires a matching resistance factor for the sake of comparison. Chapter 2 of CHBDC (2014) specifies that the designer shall consider the environmental

conditions and deterioration mechanisms for the FRP reinforcement. Clause 16.4 in Chapter 16 of CHBDC refers to durability of GFRP without considering a value for the durability factor to be taken in design. On the other hand, Clause 16.5.3 specifies resistance factors to be considered in design calculations. Such resistance factors are generally associated with uncertainty in material's mechanical properties obtained from standard mechanical test method (i.e. tensile strength test method for example). Since the publication of the previous edition of the CHBDC, it is now recognized that the variability of the strength of FRPs is affected more by environmental exposure than by geometric properties and stress levels. It is for this reason that experts in the structural use of FRP are now suggesting that the resistance factors for FRPs should be specified as products of a "material" factor and an "environmental" factor (ACI 440, 2002; Karbhari, 2000). However, Clause 16.4 in CHBDC commentaries states that findings from analyses of available data in the literature have confirmed that the concerns about the durability of GFRP in alkaline concrete, based on simulated laboratory studies in alkaline solutions, are unfounded. Thus, the resistance factor for design calculations of GFRP in CHBDC was 0.75, as given in CHBDC Commentaries, which was mainly drawn from the Japanese document (JSCE, 1997). Table 4 presents the factors of safety for the design of the proposed joint details in the tested slabs as the ratio between the experimental moment resistance and the theoretical resistance moment. As well as, the ratio between the experimental shear resistance and the theoretical shear resistance. Also, a durability factor of 0.75 is introduced to the experimental findings and the code resistance factors are applied to code theoretical equations for resisting moment and shear forces. One may observe that the factors of safety in pure shear capacity in the right column in the table are always more than 1, except for slabs S3 & S4, which have a shorter joint width. However, the factors of safety for moment are less than 1 for the jointed slabs with non-contact splices. This may be attributed to the fact that the moment capacity was calculated for the GFRP-reinforced concrete section just outside the joint considering full bond between the GFRP bars and concrete. This criteria of full bond between the bar and concrete may not be applicable since the jointed slabs with pure flexural failure exhibited very wide flexural crack at the joint-precast slab interface, indicating bar slip from UHPFRC at slab failure. Also, the factor of safety for only pure moment capacity may not apply to slabs failed in combined flexure and shear. Thus, for design purposes, the experimental findings can directly be compared to the applied factored moment in the deck slab due to dead and live loads to obtain the maximum span between girders so that researchers and engineers can implement one of the developed joint details in their projects.

Table 6: Summary of Experimental Moment and Shear Compared to Theoretical Values

Slab	Experimental Results			Theoretical Moment			Theoretical Shear		
	Failure Mode	M_{EXP}	V_{EXP}	M_r	$\frac{M_{EXP}}{M_r}$	$\frac{0.75M_{EXP}}{M_r}$	V_r	$\frac{V_{EXP}}{V_r}$	$\frac{0.75V_{EXP}}{V_r}$
		kN·m/m	*kN/m*	*kN·m*			*kN*		
S1	Flexural-Shear	128.52	116.83	89.23	1.44	1.08	64.07	1.82	1.37
S2	Flexural-Shear	128.58	116.90	89.84	1.43	1.07	64.56	1.81	1.36
S3	Flexural	69.87	63.52	89.20	0.78	0.59	64.04	0.99	0.74
S4	Flexural	85.83	78.03	89.82	0.96	0.72	64.54	1.21	0.91
S5	Flexural	110.10	100.08	90.42	1.22	0.91	65.03	1.54	1.15
S6	Flexural	107.85	98.05	89.01	1.21	0.91	63.90	1.53	1.15

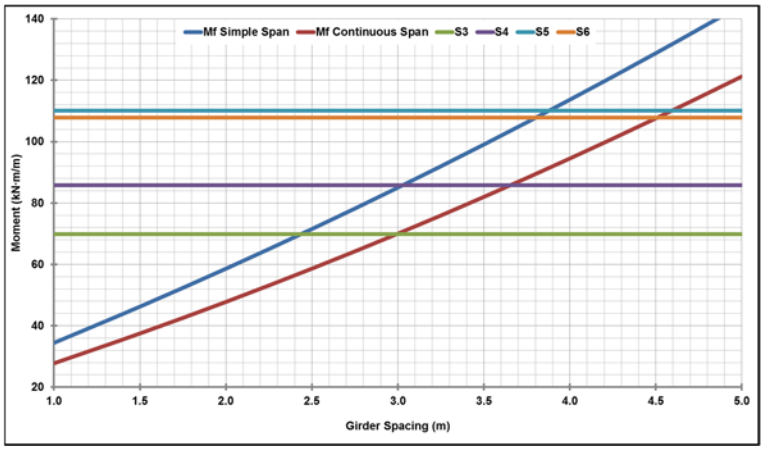

Figure 20: Specified maximum spacing between girders for jointed slabs

5.3 Design Charts for Moment Capacity

It can be observed that the slab capacity increases with increase in joint width. As such, it was decided to calculate the maximum served span between longitudinal girders in slab-on-girder bridges by comparing the applied factored moment in the deck slab due to dead and live load with the experimental values. The applied transverse live load moment for simple slab and continuous slabs were calculated according to Section 5 of CHBDC. Thus, the factored applied moment, M_f, is taken as summation of the factored dead load moment and live load moment. The factored dead load moment includes the moment from the weight of the deck slab and the asphalt layer. The slab thickness considered in this study was 200 mm with unit weight of concrete of 24 kN/m^3 and dead load factor of 1.2. The asphalt layer was assumed of 90 mm thickness and unit weight of 23.5 kN/m^3 with dead load factor of 1.5. The wheel load for live load moment calculations was 87.5 kN with dynamic load allowance of 0.4 and live load factor of 1.7. The applied factored moment in deck slab was calculated for slab spans ranging from 1 to 5.0 m with 0.5 m increments. Two deck slab conditions were considered in this study; simple span deck supported over two girders and deck slab continuous over 3 or more supports. A reduction factor of 0.8 was applied to the live load moment for continuous span deck slab per CHBDC. On the other hand a durability resistance factor of 0.75 was applied to the experimental resisting moment that was normalized to be per meter width rather than the actual slab width considered in the tested slab. Figure 18 shows comparison between the applied factored moments for simple span and continuous span deck slabs against the modified experimental findings for girder spacing ranging from 1 to 5.0 m. From the graph, limiting girder spacing was determined for each joint configuration as the point of intersection of the factored applied moment and the resisting moment obtained experimentally (Figure 20). This data was then summarized in Table 5 to assist engineers in selecting the proper joint type per the girder spacing in their bridge project. The use of this data is limited to the materials and geometric conditions in this research. Also, some potential factors of interest could not be addressed in this study. So, bridge designers are expected to include these factors in their design.

Table 5: Specified Maximum Spacing Between Girders for Jointed Slabs

Group	Slab	Splice Spacing	Main Bar Spacing	Splice Length	Joint Width	Girder Spacing Limit	
						Inner Portion of Simple Span	Inner Portion of Continuous Span
		mm	*mm*	*mm*	*mm*	*m*	*m*
2	S3	100	200	75	125	2.40	2.95
	S4			105	155	3.00	3.60
	S5			135	185	3.85	4.55
	S6			165	215	3.80	4.50

6 CONCLUSIONS

Glass fiber reinforced polymer (GFRP) bars are used in bridge decks to overcome the problem of corrosion of steel bars and concrete spalling. However, design guidelines for joints between GFRP reinforced precast deck panels supported over girders for accelerated bridge replacement is as yet unavailable. The proposed research investigates the use of GFRP bars in the closure strip between jointed precast deck panels, which is filled with ultra-high performance fiber reinforced concrete (UHPFRC). Four different bar splice lengths in the joint were considered in this study, namely: 75, 105, 135 and 165 mm. Six specimens were constructed and tested to-collapse to determine their structural behavior and load carrying capacity. Correlation between experimental findings and available design equations for moment and shear capacities was conducted, leading to recommendations for the use of the proposed joints between precast deck panels in slab-on-girder bridges. Based on experimental findings and theoretical analysis, the following conclusions can be drawn:

1- The capacity of the jointed slab increases with longer bar splice lengths in the joint. Similar conclusion can apply to the bar development length into the joint as well as the joint width.
2- With increase in bar splice length, slab failure mode changed from flexural failure due to bar slip and rib shearing in UHPFRC-filled joint to flexural-shear failure between the joint and the support

Acknowledgements

The authors would like to acknowledge the support of Fiberline Composites Canada Inc. and CRH Canada Group Inc. for this project.

References

AASHTO. 2009. AASHTO-LRFD Bridge Design Guide Specifications for GFRP-Reinforced Concrete Bridge Decks and Traffic Railings. American Association of State Highway and Transportation Officials. Washington D.C.

AASHTO. 2014. AASHTO LRFD Bridge Design Specifications. American Association of State Highway and Transportation Officials. Washington D.C

ACI 440.2R-08. 2008. Guide for the Design and Construction of Externally Bonded FRP Systems for Strengthening Concrete Structures: 45. American Concrete Institute. Farmington Hills, Michigan.

Afefy, H., Sennah, K., Tu, S., Ismail, M., and Kianoush, R. 2015. Experimental Study on the Ultimate Capacity of Deck Joints in Prefabricated Concrete Bulb-Tee Bridge Girders. Journal of Bridge Structures, Design, Assessment and Construction, 11 (2015) 55–71.

Badie, S., and Tadros, M. 2008. Full-Depth Precast Concrete Bridge Deck Panel Systems. NCHRP Report 584, Transportation Research Board, Washington, D.C.

CHBDC. 2014. Canadian Highway Bridge Design Code, CAN/CSA-S6-14. Canadian Standard Association, Toronto, Ontario, Canada.

Culmo, M. P. 2009. Connection Details for Prefabricated Bridge Elements and Systems. Report No. FHWA-IF-09-010., Federal Highway Administration, 568 pages.

Culmo, M. P. 2011. Accelerated Bridge Construction - Experience in Design, Fabrication and Erection of Prefabricated Bridge Elements and Systems. Report FHWA-HIF-12-013, Federal Highway Administration, McLean, VA, USA.

Graybeal, B. 2010. Behavior of Field-Cast Ultra-High Performance Concrete Bridge Deck Connections under Cyclic and Static Structural Loading. Federal Highway Administration, Report No. FHWA-HRT-11-023, 106 pp.

ISIS. 2007. Reinforcing Concrete Structures with Fibre Reinforced Polymers, Design Manual No.3, Intelligent Sensing for Innovative Structures, ISIS Canada. University of Manitoba, Manitoba, Canada.

JSCE. 2001. Recommendations for Upgrading of Concrete Structures with Use of Continuous Fiber Sheets. JSCE Concrete Engineering Series, Tokyo, 41: 31-34.

Karbhari, V.M. 2000. Determination of Materials Design Values for the Use of Fibre-Reinforced Polymer Composites in Civil Infrastructure. Proceedings of the Institution of Mechanical Engineers - Materials and Design. 214 (Part L): 163–171.

Khalafalla, I., and Sennah, K. 2015. Fatigue Behavior of a Developed UHPC-Filled Precast Deck Joint in Bulb-Tee Bridge Girder System Reinforced with Sand-coated GFRP Bars. Proceedings of the CSCE Annual Conference, Canadian Society for Civil Engineering, Regina, SK, pp. 1-10.

Li, L., Ma, Z., Griffey, M., Oesterle, R. 2011. Improved Longitudinal Joint Details in Decked Bulb Tees for Accelerated Bridge Construction: Concept Development, J. of Bridge Engineering, 15(3): 327-336.

NCHRP. 2011. Summary of Cast-In-Place Concrete Connections for Precast Deck Systems. Research Results Digest 355, Transportation Research Board, pp. 1-33.

PCI. 2011. PCI State-of-the-Art Report on Full-Depth Precast Concrete Bridge Deck Panels (SOA-01-1911), PCI Committee on Bridges, Precast/Prestressed Concrete Institute. Chicago, IL.

Sayed Ahmed, M., and Sennah, K. 2016. Fatigue Strength of Angle-shaped Transverse Connection for GFRP-reinfroced Precast Full-depth Deck Panels in Accelerated Bridge Construction. Proceedings of the 5th International Structural Specialty Conference, CSCE, London, Ontario, pp. 1-9.

Schoeck Canada.2013. “Schöck ComBAR technical information.” http://www.schoeck.ca (Jul. 14, 2013).

Sennah, K., and Afefy, H. 2015. Development and Study of Deck Joints in Prefabricated Concrete Bulb-Tee Bridge Girders: Conceptual Design. Journal of Bridge Structures, Design, Assessment and Construction, 11 (2015) 33–53.

Sherif, M. 2017. Flexural Strength Prediction of Closure Strip between Prefabricated Deck Slabs Supported Over Bridge Girders Incorporating GFRP Bars and UHPFRC. M.A.SC. Thesis, Ryerson University, Toronto, Ontario, Canada.

Zhu, P., Ma, Z., Cao, Q., and French, C. 2012. Fatigue Evaluation of Transverse U-Bar Joint Details for Accelerated Bridge Construction. Journal of Bridge Engineering, 17:191-200.